Supplemental material

McIntosh et al., https://doi.org/10.1083/jcb.201802138

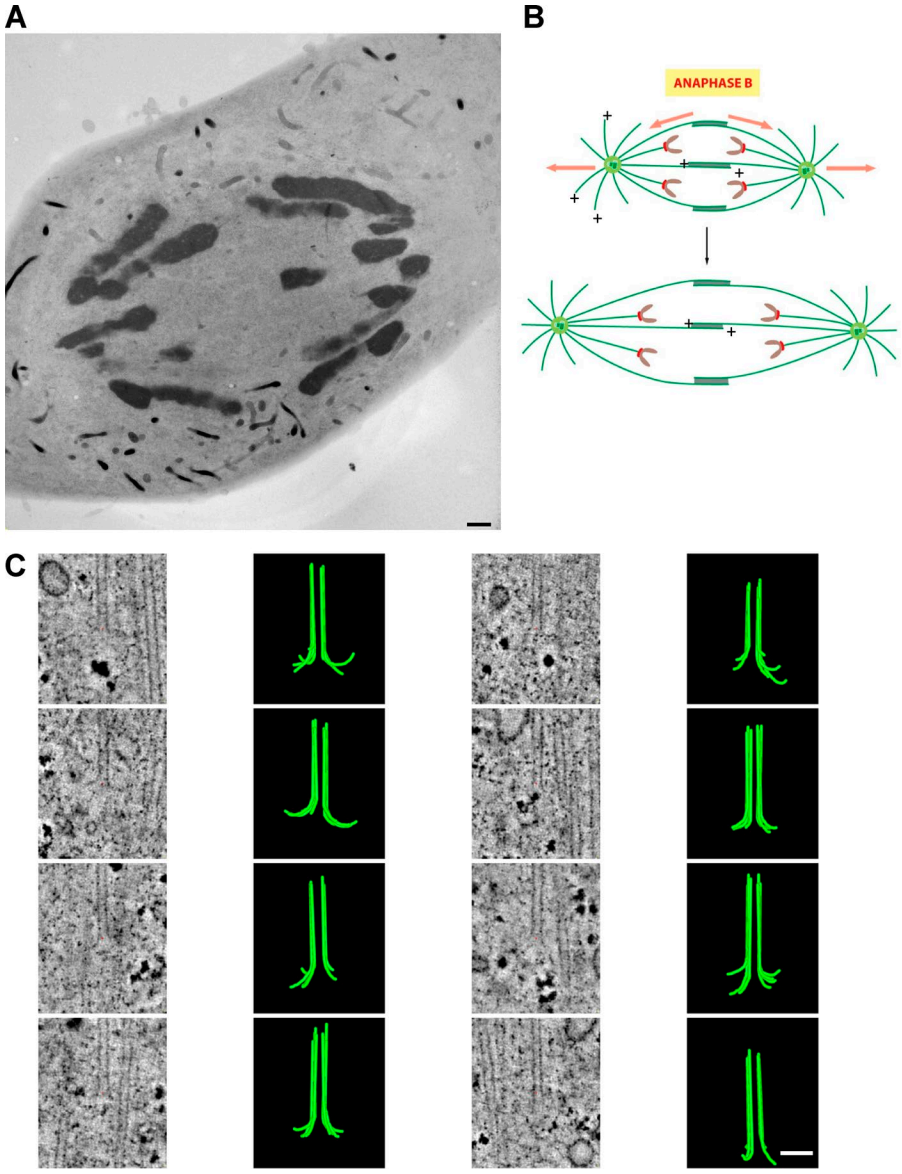

Figure S1. **Image and diagram to show the sites from which anaphase IPMTs were taken for analysis of elongating MTs and images of IPMTs from PtK_2 cells in anaphase. (A)** Thick (300 nm) section for EM of a PtK_2 cell in early anaphase B. The MTs used for study of growth morphology were taken from the midregion of this cell and others like it. IPMTs from other species came from comparable areas of anaphase spindles in those cell types. **(B)** Diagram showing the organization of IPMTs in anaphase B and the locations of plus ends, which are the sites of tubulin addition for MT growth during spindle elongation. **(C)** Gallery of IPMT ends from anaphase PtK_2 cells. Images are slices ∼4 nm thick cut from tomograms of MT ends. Models are traces drawn on the same MT ends by rotary sampling of the end structures to view as many PFs as possible. Red crosses mark the origins of the coordinate systems used. Bars, 50 nm.

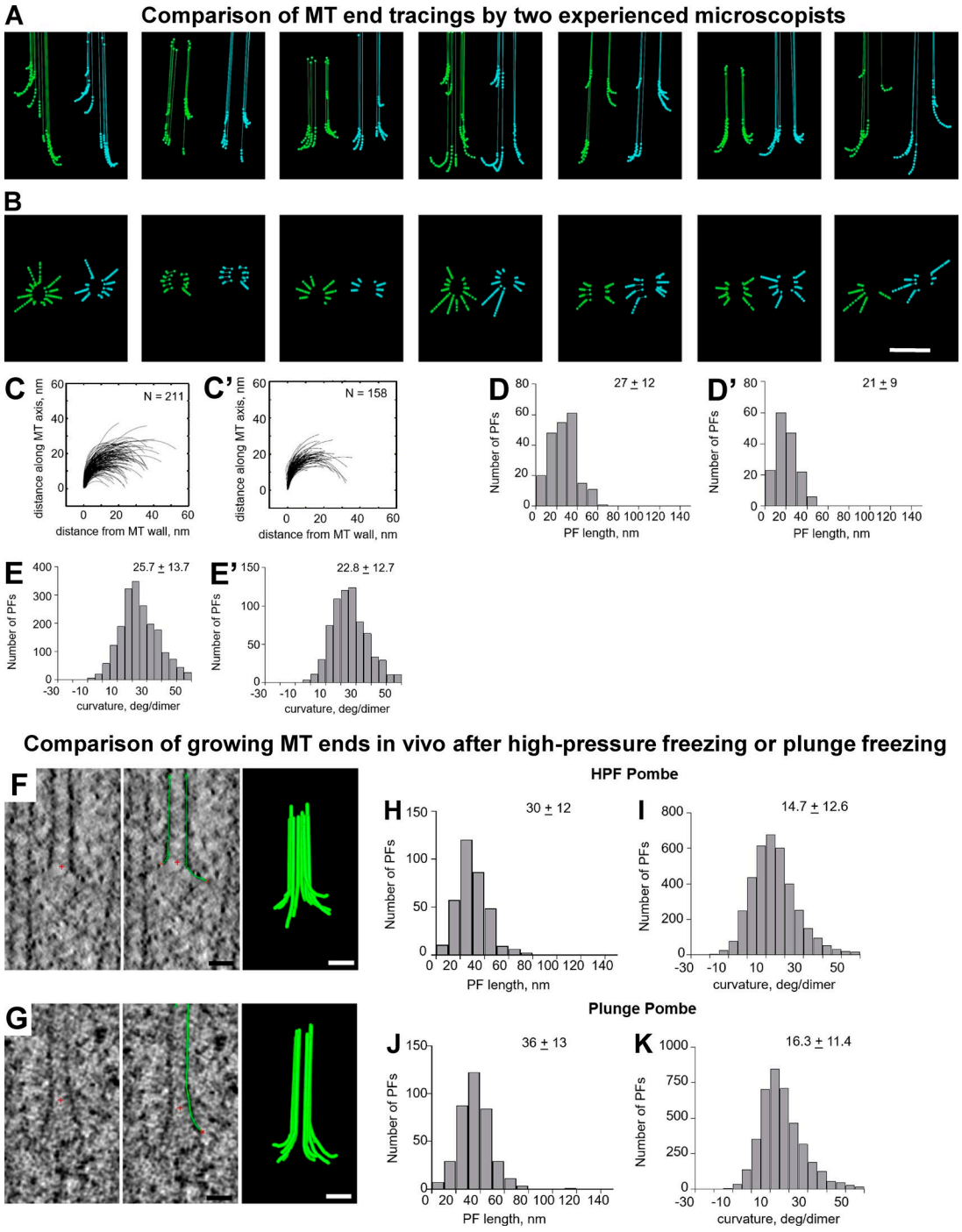

Figure S2. **Comparison of MT models traced by different observers and comparison of MT end structures in anaphase fission yeast cells prepared by high-pressure freezing or by plunging directly into liquid ethane. (A and B)** Models of the ends of four elongating MTs traced by two experienced MT trackers (J.R. McIntosh, green traces; E. O'Toole, blue traces). The two sets of models show the similarity between PF traces when the MTs are properly aligned in the coordinate system for rotational analysis. The models are not identical because the different trackers did not identify all the same PFs. They are, however, similar, encouraging confidence in the validity of the hand-drawn traces. **(C and C')** Drawings of all PFs traced by the two modelers on the same dataset. J.R. McIntosh found more PFs thanks to his making drawings on slices cut at higher angles. N, numbers traced. **(D and D')** Distributions of PF lengths from the two sets of traces. J.R. McIntosh's traces are more numerous and slightly longer. **(E and E')** Distributions of angles from the two sets of traces. The distributions are very similar. **(F)** End of a growing IPMT from a fission yeast cell prepared by high-pressure freezing (HPF). Left: Tomographic slice that contains the MT axis. Middle: The same slice with an overlay of the graphic objects used to represent the PFs visible in this slice. Right: Model of all PFs visible on this MT end using rotational sampling. **(G)** The same set of images as F for a comparable MT from the interzone of a cell prepared by plunge freezing. Red crosses mark the origins of the coordinate systems used. Bars, 25 nm. **(H and J)** Distributions of lengths for all PFs digitized in fission yeast cells prepared by these two methods of freezing as marked. **(I and K)** Distribution of PF curvatures from cells prepared these two methods of freezing as marked. Numerical values for means, modes, and SD are shown in Table 1. Pombe, *S. pombe*.

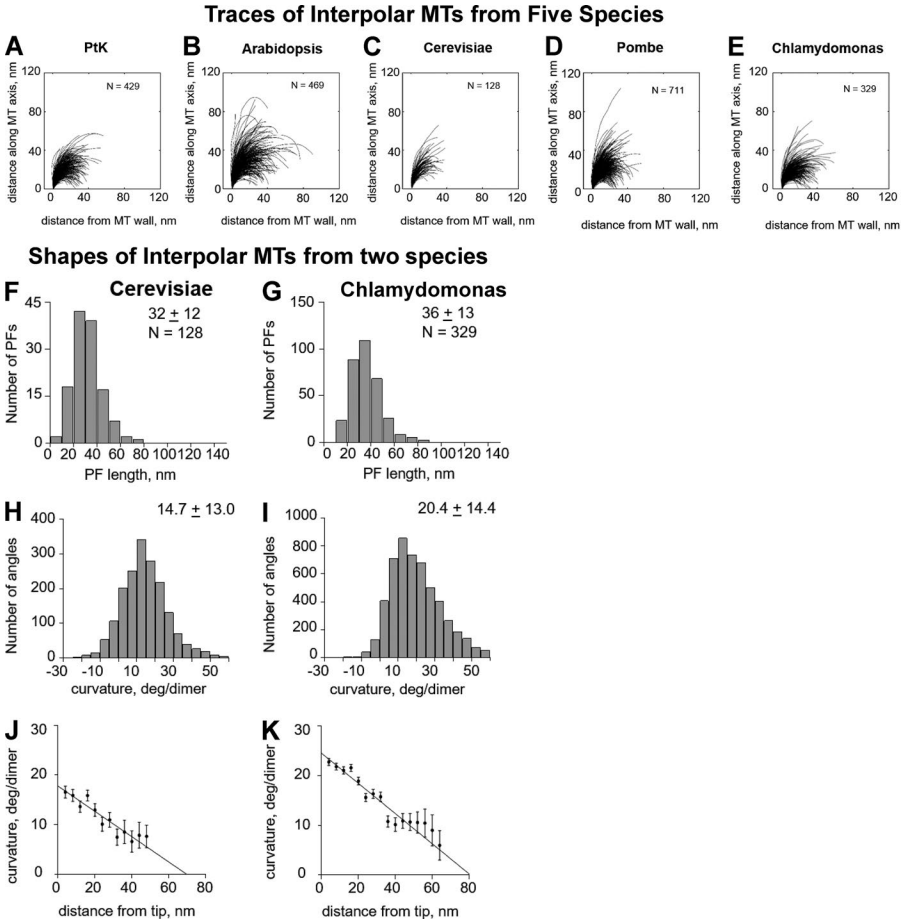

Figure S3. **Traces of PFs on anaphase IPMTs from five species and distributions of PF shape parameters for anaphase IPMTs from *S. cerevisiae* and *Chlamydomonas*. (A–E)** The flaring portions of all PFs traced for all anaphase IPMTs are shown for each species. The numbers of PFs are shown in each drawing, and the mean lengths and curvatures for all PFs from each cell type are shown in Table 1. Pombe, *S. pombe*. **(F and G**) Distributions of PF lengths for these two species. N, number of PFs traced. Data are means ± SD. **(H and I)** Distributions of angles for the same PFs. **(J and K)** Graphs of the mean curvatures and SEM for all these PFs plotted as a function of distance from the PF tips.

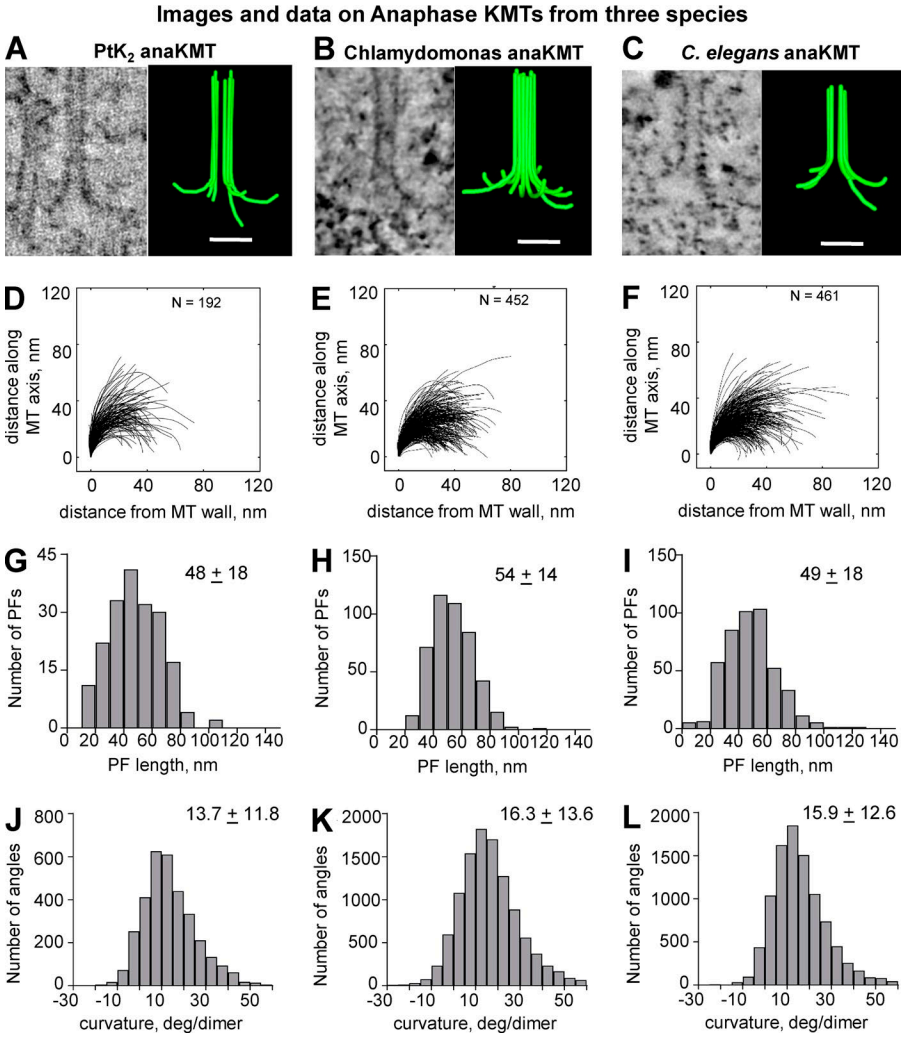

Figure S4. **Images and data describing the shapes of KMT plus ends in anaphase from three species. (A–C)** Images of slices from tomograms and models of representative KMTs from PtK_2 cells, *Chlamydomonas*, and *C. elegans*. Bars, 50 nm. **(D–F)** Tracings of PF shapes for anaphase KMTs from each of these species. N, numbers traced. **(G–I)** Distributions of lengths for all PFs traced on anaphase KMTs from each species. **(J–L)** Distributions of angles for all PFs traced on the same MTs from each species.

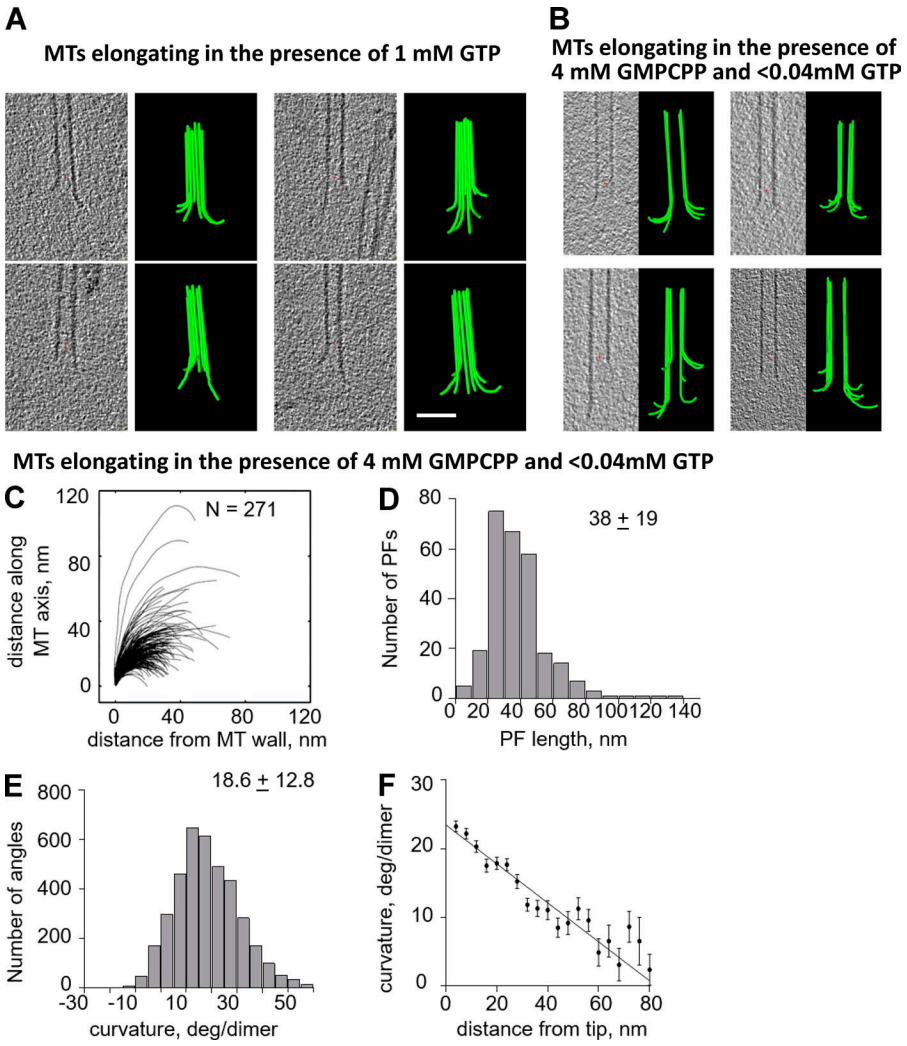

Figure S5. **Gallery of images, models, traces, and data analyses for PFs at the ends of MTs growing in vitro in either 1 mM GTP or 4 mM GMPCPP and trace GTP. (A)** Four MT ends are represented by a tomographic slice that contains the MT axis and a model of all the PFs drawn on that MT end with the aid of rotary sampling. **(B)** Ends of four MTs grown in buffers where the concentration of GMPCPP exceeded that of GTP by >100-fold. The ends are represented by a tomographic slice that contains the MT axis and a model of all PFs drawn on that MT end with the aid of rotary sampling, showing the shape of MTs. Red crosses mark the origins of the coordinate systems used. Bar, 50 nm. **(C–F)** Traces and data describing the PFs on GMPCPP-grown MTs as indicated. N, numbers traced. F displays mean curavtures and SEM of those curvatures as a function of position.

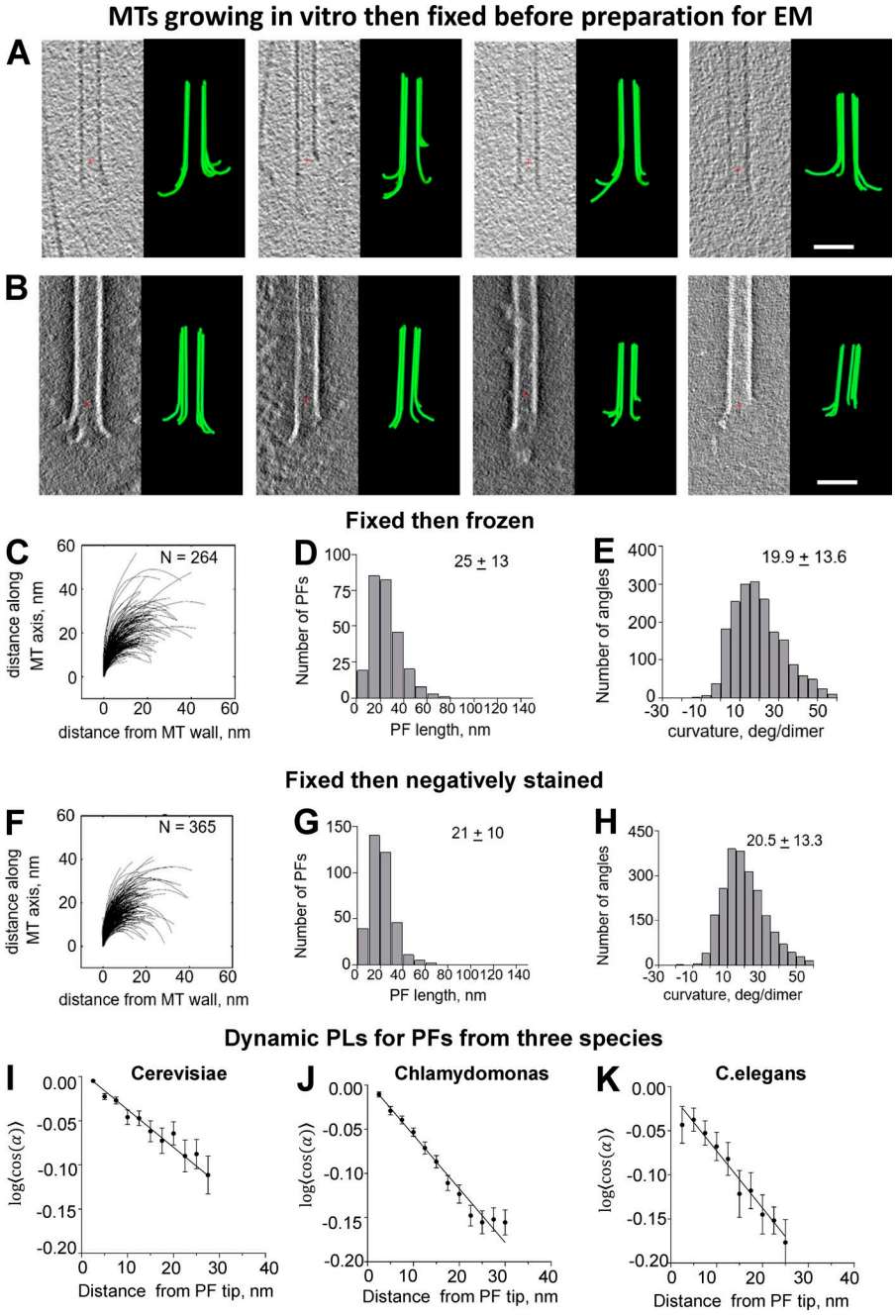

Figure S6. **Images, models, and data describing the ends of MTs grown in GTP and then fixed in glutaraldehyde before either rapid freezing or negative staining as well as data that characterize the flexibility of PFs on IPMTs from three species. (A)** Ends of MTs fixed in 0.2% and then 2% glutaraldehyde and then rinsed in BRB80, blotted, and frozen by plunging in liquid ethane. **(B)** Ends of MTs fixed in 0.2% and then 2% glutaraldehyde and then negatively stained in 2% uranyl acetate, blotted, and air dried for ET. Red crosses mark the origins of the coordinate systems used. Bars, 50 nm. **(C–H)** Traces and distributions of lengths and angles for these two samples of growing MT ends as indicated. N, numbers traced. **(I–K)** Plots that reflect the mean deviation and SEM for each set of PFs from the mean curvature at that point for that set of PFs as a function of distance from the PF tip. The resulting values of dynamic persistence length are shown in Table 4.

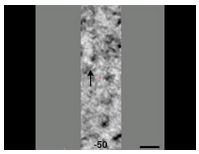

Video 1. **Rotary sampling of the end of an IPMT from the anaphase B interzone of a PtK$_2$ cell.** The view under examination was framed to include one MT end, and then the Slicer module of IMOD was used to orient the plane of sampling to contain the MT axis. The plane of view was then rotated about the MT axis up to 50°. A JPG image was recorded, the angle was changed by 2°, and another image was recorded, etc., until the entire useful range of sampling of the tomographic volume had been recorded. During this process, the previously drawn model of the MT end was turned on and off to display the recording of PF shape and position that had previously been done. This set of JPG images was then made into the video shown using QuickTime Pro. Arrows have been added to indicate places where we saw curving PFs. Careful viewing of this video will show both how clear some PFs are and how others are not so clear. In making our choice about what to trace and how to do it, we examined the full range of tilts and used the 13-fold symmetry of MTs to guide some of the choices about what structures to trace. Another experienced observer might have chosen somewhat different PF-like objects to trace, but we are confident that our models are valid representations of all general aspects of MT end structure.

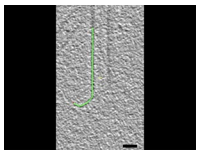

Video 2. **Rotary sampling of the end of an elongating MT growing from an outer-doublet MT from an axoneme of *Chlamydomonas*.** The video of this kind of MT was made as described for Video 1. Arrows indicate curving PFs.

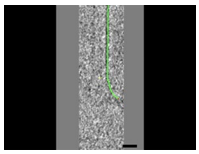

Video 3. **Rotary sampling of the end of an elongating MT growing from an outer-doublet MT from an axoneme of *Chlamydomonas* in the presence of 100-fold excess GMPCPP.** The video of this kind of MT was made as described for Video 1. Arrows indicate curving PFs.

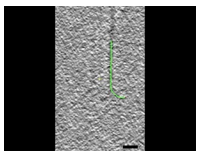

Video 4. **Rotary sampling of the end of an elongating MT that was fixed and then frozen.** The video of this kind of MT was made as described for Video 1. Arrows indicate curving PFs.

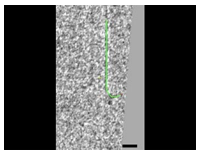

Video 5. **Rotary sampling of the end of a shortening MT that initially grew from an outer-doublet MT from an axoneme of *Chlamydomonas*.** The video of this kind of MT was made as described for Video 1. Arrows indicate curving PFs.

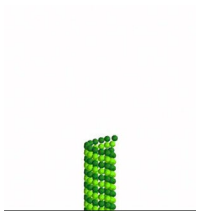

Video 6. **Coarse-grained molecular dynamics showing MT growth by a mechanism that relies on thermal fluctuations of PFs to straighten these elongating oligomers.** α-Tubulins are shown in lighter green, and β-tubulins are shown in darker green. Total simulation time shown in the video is ∼1.7 s. Video is played 50× slower than model time.